

Engineering of Landau–Zener tunneling

G. Tayebirad · R. Mannella · S. Wimberger

Received: 29 June 2010 / Revised version: 30 September 2010 / Published online: 11 February 2011
© Springer-Verlag 2011

Abstract Several ways are discussed to control the Landau–Zener tunneling in the Wannier–Stark system. We focus on a realization of this system with interacting and noninteracting ultracold bosons. The tunneling from the ground band to the continuum is shown to depend crucially on the initial condition and system parameters and, more interestingly, on added time-dependent disorder—noise—on the lattice beams.

1 Introduction

Bloch oscillations, Landau–Zener (LZ) tunneling, and Wannier–Stark ladders [1–11], are fundamental quantum effects occurring in a system of electrons moving in a periodic potential and subjected to a constant electric field. Due to complications such as impurities, lattice vibrations, and multiparticle interactions, clean observations of these effects have been difficult [12]. In recent years, ultra-cold atoms and Bose–Einstein condensates in optical lattices have been increasingly used to simulate solid state systems and the above mentioned phenomena [6–10, 13–17]. Optical lattices are

nowadays easy to realize in the laboratory, and their parameters can be perfectly controlled both statically and dynamically, which makes them attractive model systems for crystal lattices. More complicated potentials can be realized by adding further lattice beams [18–24]. In fact, by superimposing laser beams from different directions and with slightly different wave-lengths, it is possible to generate many different three-dimensional lattice geometries [16, 17]. The question arises of how to control the dynamics of particles by quasi-periodic potentials (possibly time-dependent or even stochastic ones).

In this paper, we present results on the Wannier–Stark system realized with ultracold atoms, forming a Bose–Einstein condensate, in an optical lattice [6–10, 14, 25–29]. We compute the time dependence of the tunneling probability of the Bose–Einstein condensate atoms out of the ground band in which they were originally prepared. By changing the initial condition and the system parameters and introducing atom–atom interactions into the system, we are able to control the tunneling rate of the Bose–Einstein condensate to higher bands. Finally, a controlled noise added to the system will be shown to be a further handle to engineer the interband tunneling.

2 Landau–Zener tunneling in optical lattices

We study the temporal evolution of ultracold atoms loaded into a quasi one-dimensional optical lattice which can be a spatially periodic potential or a time-dependent stochastic potential, subjected to an additional static force, in the presence of weak atom–atom interactions [29]. We use the following general form of the three-dimensional Gross–Pitaevskii equation to model the temporal evolution

G. Tayebirad (✉) · S. Wimberger
Institut für Theoretische Physik, Universität Heidelberg,
Philosophenweg 19, 69120 Heidelberg, Germany
e-mail: g.Tayebirad@thphys.uni-Heidelberg.de

R. Mannella
CNR-INFN and Dipartimento di Fisica ‘E. Fermi’,
Università di Pisa, Largo Pontecorvo 3, 56127 Pisa, Italy

S. Wimberger
Center for Quantum Dynamics, Universität Heidelberg,
Heidelberg, Germany

of the atoms

$$H = -\frac{\hbar^2}{2M} \nabla_{\vec{r}}^2 + W(\vec{r}, t) + g_{3D} |\Psi(\vec{r}, t)|^2 + Fx; \quad (1)$$

$$W(\vec{r}, t) = V_{\text{trap}}(\vec{r}) + V_1(x) + V_2(x, t),$$

with lattice potentials along the longitudinal direction, x , as

$$V_1(x) = \alpha V \sin^2\left(\frac{\pi x}{d_L}\right); \quad (2a)$$

$$V_2(x, t) = \alpha V \sin^2\left(\frac{\pi x}{d'_L} + \phi(t)\right). \quad (2b)$$

M is the mass of condensate atoms and F is the Stark force. $V_1(x)$ and $V_2(x, t)$ are spatially periodic potentials with incommensurate lattice spacings d_L and d'_L , respectively. As will be shown below around (9), the noise has a tendency to average over the second lattice, and therefore the amplitudes of the two lattices should be comparable. For convenience we chose equal amplitudes αV and $d_L = 426$ nm and $d'_L = d_L(\sqrt{5} - 1)/2$ for the lattice constants. The potential $V_2(x, t)$ is a time-dependent stochastic potential with a time-dependent stochastic phase $\phi(t)$, which we will characterize further down in Sect. 2.2. The renormalization factor α is introduced to be able to compare the dynamics in the presence of the potential given by (2a) and (2b) to the dynamics of the “reference system”, i.e. the dynamics in the potential $W(\vec{r}) = V_{\text{trap}}(\vec{r}) + V \sin^2(\frac{\pi x}{d_L})$. α will be chosen in such a way that the following standard deviations are equal:

$$\left\langle \left(\left\langle \sin^2\left(\frac{\pi x}{d_L}\right) \right\rangle_x - \left\langle \sin^2\left(\frac{\pi x}{d'_L}\right) \right\rangle_x \right)^2 \right\rangle_x = \left\langle \left(V_{\text{eff}}(x) - \langle V_{\text{eff}}(x) \rangle_x \right)^2 \right\rangle_x, \quad (3)$$

where the effective potential $V_{\text{eff}}(x)$ will be defined in Sect. 2.2. The average $\langle \cdot \rangle$ is an integral over space for a sufficiently large L , i.e., $\langle \cdot \rangle = 1/L \int_{-L/2}^{L/2} dx$. The third term in the Hamiltonian is the non-linearity, which makes the equation different from the Schrödinger equation. $\Psi(\vec{r}, t)$ represents the condensate wave function and $|\Psi(\vec{r}, t)|^2$ the local atomic density. $g_{3D} = \frac{4\pi\hbar^2 a_s N_0}{M}$ is the coupling constant which is proportional to the scattering length a_s and determines the strength of atom–atom interactions, where $\frac{4\pi\hbar^2 a_s}{ME_R} \approx 2.45 \times 10^{-21} \text{ m}^3$, with $a_s = 53 \times 10^{-10} \text{ m}$ and $M = 1.44 \times 10^{-25} \text{ kg}$ for rubidium 87. N_0 is the number of atoms in the condensate. The recoil energy $E_R = p_R^2/2M$ and the recoil momentum $p_R = \pi\hbar/d_L$ are the characteristic energy and momentum scales for our system. Moreover, we define $V_0 = V/E_R$ and $F_0 = Fd_L/E_R$ as dimensionless quantities in this energy unit. Experimentally, the

initial state is the relaxed condensate wave function prepared in the confining potential given by a harmonic trap $V_{\text{trap}} = \frac{1}{2}m(\omega_\rho^2 \rho^2 + \omega_x^2 x^2)$, with $\omega_x \ll \omega_\rho$ for a quasi 1D situation, and then loaded adiabatically into the optical lattice when the Stark force F equals zero. Then ω_x is either switched off or relaxed to a small value $\omega_{x,\text{rel}}$ and the Stark force F is simultaneously switched on to induce the dynamics. In the following sections we study the system in the presence/absence of different terms of the above Hamiltonian.

2.1 Noise free case

2.1.1 Linear case—Wannier–Stark problem

For zero or small $\omega_{x,\text{rel}}$ (cf., e.g., [30]) and negligible atom–atom interactions, when $V_2(x, t) = 0$ and $\alpha = 1$, the above Hamiltonian in (1) describes the dynamics of atoms in a tilted periodic potential which is the well-known single-particle Wannier–Stark problem. Without the non-linearity term, we can use the 1D version of (1) for our simulations. In the presence of F , the quasimomentum of a condensate (initially prepared at the center of the Brillouin zone in the ground band) scans the lower band in an oscillating motion periodically—so-called Bloch oscillations—with the Bloch period $T_B = 2\hbar(Fd_L)^{-1}$. At the edge of the Brillouin zone, where the gap between the ground and the first excited band ΔE of the $F = 0$ system (increasing with V_0 [31]), acquires its minimum value, a tunneling of the condensate to the first excited energy band may occur. The tunneled atoms escape from the system through successive tunneling events across the much smaller band gaps between the upper bands. This phenomenon is known as the LZ tunneling. LZ theory predicts a decay rate

$$P_{\text{LZ}} = e^{-\frac{\pi}{\gamma}}, \quad (4)$$

where γ is the adiabaticity parameter and $\gamma \approx \frac{32F_0}{\hbar V_0^2}$ [31]. In order to study the LZ prediction for our system we need to access the decay rate of the population from the ground band. In that respect, we compute the time dependence of the probability of the condensate to remain in the ground band in which it has been initially prepared. Such a survival probability is best measured in momentum space. From the time-dependent momentum distribution we can determine $P_{\text{sur}}(t)$ by projection of the evolved state $\tilde{\Psi}(\vec{p}, t)$ on to the support of the initial state [30, 32, 33]

$$P_{\text{sur}}(t) = \int_{-\infty}^{\infty} \int_{-\infty}^{\infty} dp_y dp_z \int_{-p_c}^{\infty} dp_x |\Psi(\vec{p}, t)|^2, \quad (5)$$

where p_c is an ad hoc cut-off momentum. In our calculation we chose $p_c = 3p_{\text{rec}}$. Then (5) starts to measure the

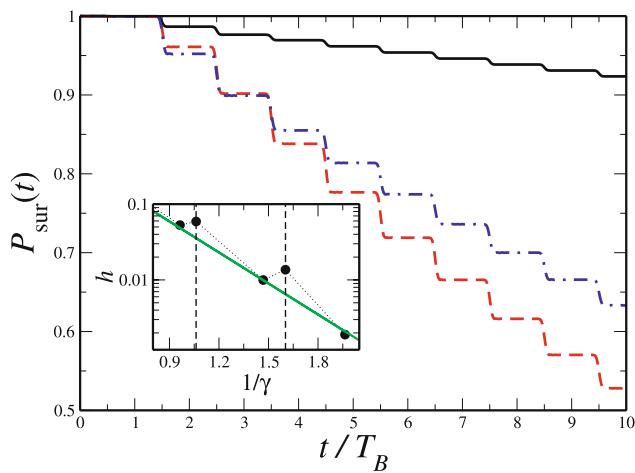


Fig. 1 Time-resolved survival probability of the BEC in the ground band, for a lattice depth $V_0 = 4$, and a narrow width of the initial momentum distribution of the BEC cloud, $\Delta p/2p_R = 0.05$ (trap frequency $\omega_x = 2\pi \times 50$ Hz), and various Stark forces. For non-RET condition: $F_0 = 1.07$ (solid line) and $F_0 = 1.63$ (dash-dotted line); for RET condition: $F_0 = 1.48$ (dashed line). *Inset:* height of one step (of data as shown in the main panel) for fixed $V_0 = 4$ and various γ . The step height as predicted by (4) (solid line) in comparison with the numerically obtained values (filled circles). A significant deviation from the LZ prediction can be observed at values of $\frac{1}{\gamma}$ corresponding to RET conditions and marked by the vertical dashed lines

wave packet leaving the ground band with an artificial delay of one Bloch period, since by the acceleration theorem the average momentum is proportional to time (more details can be found in [30, 32, 33]). A very nice step structure—local deviation from the overall exponential decay—can be seen in the survival probability (see Figs. 1 and 2). Such step structures reflect the above mentioned phenomena, i.e., Bloch oscillations and LZ tunneling. One can see that the tunneling events from the ground band to the next band occur after each Bloch period when the wave packet is at the edge of the Brillouin zone. It is possible to control the LZ tunneling of the Bose–Einstein condensate from the ground band in the linear system and in the absence of atom–atom interactions by

- Changing the system parameters, such as external force F_0 , and the amplitude of the optical lattice V_0 (see Fig. 1)
- Exploiting resonantly enhanced tunneling (RET) between degenerate Wannier–Stark states at $\Delta E \approx n \times Fd_L$ with n being an integer number (see Fig. 1) [11]
- Changing the initial condition by changing the trap frequencies and hence preparing the Bose–Einstein condensate with different widths Δp of its initial momentum distribution (see Fig. 2)

As seen in Fig. 1, increasing the tilting force leads to more and more tunneling of the atoms from the ground band. On the other hand, depending on the system parameters, one can tune into a special condition for which the rate of the tunnel-

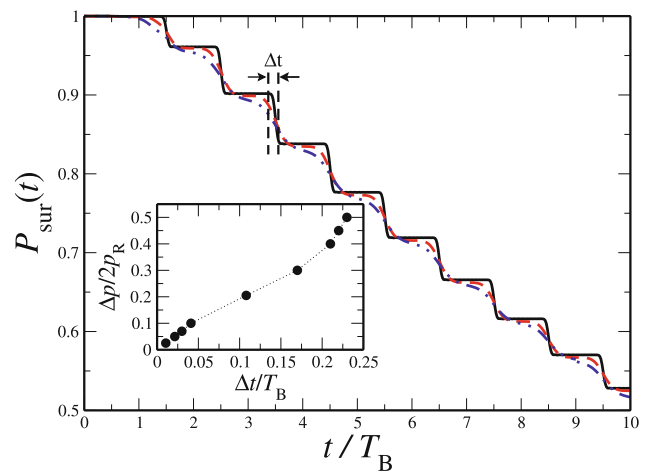


Fig. 2 The survival probability of the BEC in the ground band for a lattice depth $V_0 = 4.0$, a constant Stark force $F_0 = 1.48$, and various widths of the initial momentum distribution of the BEC cloud, $\Delta p/2p_R = 0.05$ (solid line); $\Delta p/2p_R = 0.2$ (dashed line); $\Delta p/2p_R = 0.3$ (dash-dotted line). *Inset:* step width Δt for several Δp (filled circles). The step width Δt is the distance between the two vertical dashed lines shown in the main panel for the case of $\Delta p/2p_R = 0.05$

ing is enhanced. This occurs when an integer multiple of the energy scale of the tilting force Fd_L matches the energy difference between the initial state and the final state, i.e., approximately the band gap ΔE . This phenomenon has been observed experimentally [27, 28] and is called resonantly enhanced tunneling (RET). A deviation from the LZ prediction is expected in this case. In order to see whether the tunneling probability given by the standard LZ tunneling probability correctly predicts the height of a step corresponding to a single tunneling event, we fit a step function to our step-like survival probability and extract the height of each step. The result and the comparison to the LZ prediction is shown in the inset of Fig. 1. When the system parameters are in the RET condition (e.g., $1/\gamma \approx 1.05$ and 1.6), the height of the steps of the survival probability increases and shows a significant deviation from the LZ prediction given in (4). This behavior is seen in Fig. 1 where the survival probability for $F_0 = 1.48$ decays much faster than for the other two cases. Since the derivation of (4) [31] does not take into account the actual Wannier–Stark level structure, which is necessary to describe the RET condition, (4) or the survival probability derived from it cannot describe the enhancement of the tunneling probability due to RET.

The other parameter which can affect the survival probability is the width Δp of the initial momentum distribution. By changing the trap frequencies ω_x and ω_ρ one can prepare the initial distribution with different widths. Figure 2 demonstrates the dependence of the width of the steps Δt on Δp . The steps are smooth and partly washed out since the wave packet reaches the edge of the Brillouin zone earlier

when it has a broader initial momentum distribution. Still the remnants of the steps cause a local deviation from the exponential decay of the tunneling probability. Nevertheless, the survival probability exhibits an exponential decay globally in time, i.e., on large time scales, for all the mentioned cases.

2.1.2 Non-linear case—Gross–Pitaevskii equation

In the regime of weak atom–atom interactions the effect of interactions is studied in the mean-field regime based on the Gross–Pitaevskii equation. The 3D Gross–Pitaevskii equation can describe the dynamics of the entire Bose–Einstein condensate in terms of an equation of motion for a single-particle wave function. Therefore, the following non-linear equation describes the dynamics of interacting Bose–Einstein condensate atoms in a tilted periodic potential ($V_2(x, t) = 0$) with $\alpha = 1$:

$$H = -\frac{\hbar^2}{2M} \nabla_{\vec{r}}^2 + V_{\text{trap}}(\vec{r}) + V_1(x) + g_{3D} |\Psi(\vec{r}, t)|^2 + Fx. \tag{6}$$

As mentioned in Sect. 2, g_{3D} is the coupling constant calculated from the s-wave scattering wavelength a_s and the number of atoms in the condensate N_0 . $|\Psi(\vec{r}, t)|^2$ is the local atomic density. As an estimate for the non-linear term in (6), we define $C \equiv \frac{g_{3D} |\Psi(\vec{r}, t)|^2_{\text{peak}}}{E_R}$ at the peak density of the initial state. The following effects can be seen by increasing the strength of a repulsive non-linearity ($g_{3D} > 0$) in the system:

- Enhancement of the tunneling rate
- Deviation from mono-exponential decay
- Washed out steps (corresponding to damped Bloch oscillations)

According to our results shown in Fig. 3 for a RET case and the experimental results in [27, 28], the temporal behavior of the survival probability depends on the strength of atom–atom interactions. As can be found with more detail in [27, 30], the enhancement of decay rate is generic for repulsive interactions. The scaling of the decay rate as a function of non-linearity is yet more interesting in the RET case (see the inset of Fig. 3). We can quantify the decay rate Γ of the survival probability by globally fitting an exponential decay function to the step-like curves of the survival probability. Such rates, for various non-linearities, are depicted in the inset of Fig. 3. A repulsive interaction initially enhances the interband tunneling probability of the ultracold atoms [30]. Since the tunneling events occurring at different integer multiples of the Bloch period are correlated by the presence of the non-linearity, a clear deviation from the mono-exponential decay is observed making the definition

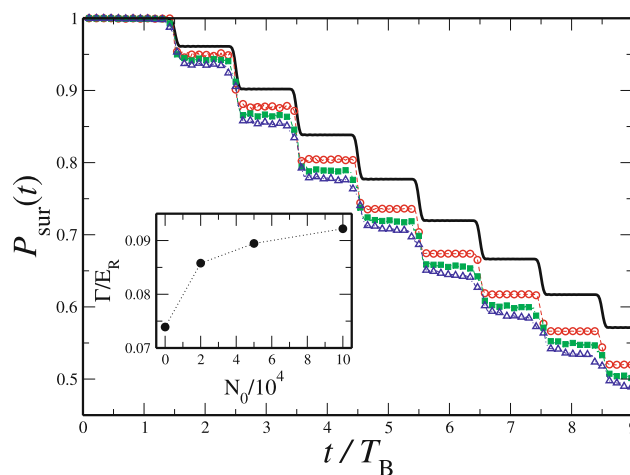


Fig. 3 Time-resolved survival probability in the ground band for the non-linear case with $V_0 = 4.0$, $F_0 = 1.48$ (RET), a narrow width of the initial momentum distribution of the BEC cloud, $\Delta p/2p_R = 0.05$, and composed of the following number of atoms prepared in a trap with $\omega_x = 2\pi \times 50$ Hz and $\omega_y = 2\pi \times 100$ Hz: $N_0 = 2 \times 10^4$, $C \approx 0.2$ (open circles); $N_0 = 5 \times 10^4$, $C \approx 0.32$ (filled squares); $N_0 = 1 \times 10^5$, $C \approx 0.42$ (open triangles) as compared to the linear case $g_{3D} = 0$, (solid line). Inset: Decay rate of the survival probability Γ at RET condition vs. N_0 (filled circles)

of a global decay rate Γ somewhat problematic [34]. A continuous change in the density of the condensate in time due to escaped particles from the system leads to a decreasing impact of the non-linearity. Therefore, the time local rate of decay systematically decreases as the time increases. Additionally, the non-linearity leads to a dephasing and damping of the Bloch oscillations, not discussed here, but a discussion of this phenomenon can be found in [14–16, 35, 36].

2.2 Impact of a time-dependent stochastic potential (noisy Wannier–Stark problem)

Going back to the linear system, $g_{3D} = 0$, the case of $V_2(x, t) \neq 0$ leads to a time-dependent stochastic potential where we claim that we are able to control the dynamics of the Bose–Einstein condensate atoms by changing the characteristic parameters of the time-dependent stochastic phase $\phi(t)$. α is no longer 1 and we can calculate it as defined above by (3), using the effective potential introduced below in (9). We use correlated noise for the time-dependent phase $\phi(t)$ for the second lattice. A standard example is exponentially correlated noise, which is characterized by a single correlation time. Such a noise can be obtained from linearly filtered white noise as

$$\dot{\phi} = -\frac{\phi}{\tau} + \frac{\sqrt{2D}}{\tau} \xi(t), \tag{7}$$

where ξ is a Gaussian white noise with zero mean and standard deviation equal to one. τ is the correlation time of the

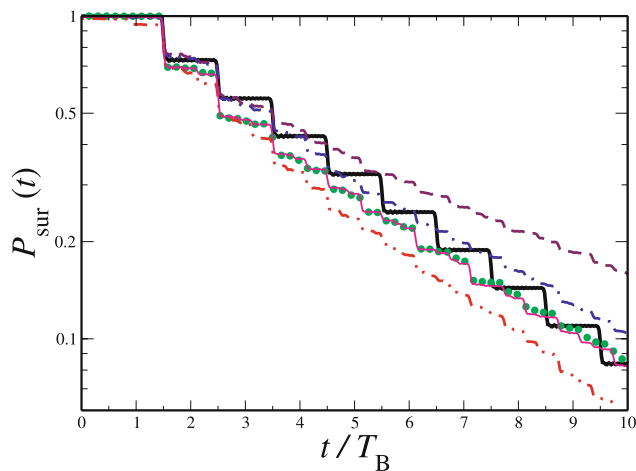


Fig. 4 Time evolution of the survival probability for $V_0 = 2.5 E_R$, $F_0 = 1.5$, and $\alpha \approx 0.82$; The thick solid line is the decay of the reference system defined by (1) with $g_{3D} = 0$, $V_2(x, t) = 0$ and $\alpha = 1$; in the presence of exponentially correlated noise with $D/\tau \approx 0.25$ and correlation times: $\tau = 10 T_B$ (dashed line), $\tau = 1 T_B$ (dot-dashed line), $\tau = 0.05 T_B$ (dot-dot-dashed line), $\tau = 0.001 T_B$ (thin solid line); results for the effective potential of (9) are shown by the filled circles

noise and the strength of the noise is given by the parameter D . The introduced noise has a zero mean ($\langle \phi(t) \rangle = 0$) and an exponential correlation function $\langle \phi(t)\phi(s) \rangle = D/\tau \exp(-|t - s|/\tau)$. τ describes the time-scale of the fluctuations and D/τ its variance. The power spectrum of the exponentially correlated noise is given by a Lorentzian function as

$$S(\omega) = \frac{D}{\pi(1 + \omega^2\tau^2)}. \tag{8}$$

Figure 4 demonstrates the survival probability of the atoms in the ground band for various correlation times τ and a fixed value of the variance $D/\tau \approx 0.25$ of the noise. The system parameters are $V_0 = 2.5 E_R$ and $F_0 = 1.5$ (non-RET condition). The solid line shows the time evolution of the survival probability for the reference system introduced by (1) with $g_{3D} = 0$, $V_2(x, t) = 0$ and $\alpha = 1$. A nice step structure similar to the ones depicted in Figures 1 and 2 is observed for this case. The other curves in Fig. 4 exhibit the time evolution of the survival probability for the temporally disordered system introduced in (1) with $g_{3D} = 0$, $V_2(x, t) \neq 0$ and $\alpha \neq 1$. As seen for all the cases the step structure is washed out. Considering the characteristic parameters of the exponentially correlated noise, different regimes of the noise are introduced. The regime of slowly varying noise is recovered when the noise has a large correlation time compared with the time scales of the system (e.g., T_B). The tunneling probability of the atoms in such a regime is suppressed (e.g., for $\tau = 10 T_B$ shown by the dashed line in Fig. 4). Decreasing the correlation time the rate of tunneling increases but, nevertheless, for $\tau \geq T_B$ the noise suppresses the tunneling compared with the reference system (see the data for

$\tau = 1 T_B$ as shown by the dot-dashed line in Fig. 4). For correlation times smaller than T_B , the noise recovers the regime of fast noise (e.g., for $\tau = 0.05 T_B$) and causes an enhancement in the tunneling rate (dot-dot-dashed line) compared with the reference system (thick solid line). Surprisingly a further decrease of the correlation time decreases the tunneling rate of the atoms (e.g., for $\tau = 0.001 T_B$ depicted by the thin solid line).

In order to understand the effect of the time-dependent stochastic potential on the system, we renormalize the potential. The time-dependent potential can be replaced by a suitable static effective potential in the limit of small τ . Such an effective potential can be calculated integrating over all possible phases giving:

$$V_{\text{eff}}(x) = \alpha V[\sin^2(\pi x/d_L) + \beta \sin^2(\pi x/d'_L)], \tag{9}$$

with a renormalization factor for the second lattice $\beta = e^{-2D/\tau}$. Equation (9) provides a time-independent potential which can be used to compute α as stated in (3). As seen in Fig. 4 the survival probability for a small $\tau = 0.001 T_B$ (thin solid line) shows perfect agreement with the results achieved using the effective potential of (9) (filled circles).

Keeping the noise parameters constant, we study the decay rate of the survival probability, Γ , of the condensate for various system parameters. The results of a scan over the Stark force are shown in Fig. 5(a). The simulations have been done for three values of the correlation time of the noise $\tau = 0.0005, 0.05, 50 T_B$, keeping the variance of the noise constant (here $D/\tau \approx 0.25$). The three correlation times are chosen from the left shoulder, the peak point and the right shoulder of curves in Fig. 5(b). The solid line depicts the decay rate of the reference system (given by (1) with $g_{3D} = 0$, $V_2(x, t) = 0$ and $\alpha = 1$). Noise in the system leads to a washing out of the RET peaks (present in the solid line of Fig. 5(a)) in the decay rate, and, dependent on the correlation time of the noise, a suppression (for very large and very small values of τ) or an enhancement of the tunneling (e.g., for $\tau \approx 0.05 T_B$) can be obtained.

We also ran a scan over the correlation time of the noise τ , again keeping the variance of the noise constant ($D/\tau \approx 0.25$). The decay rate of the survival probability for three amounts of the Stark force ($F_0 = 0.95, 1.25, 1.5$) is shown in Fig. 5(b). Comparing the symbols to the lines (which specify the decay rate in the corresponding reference system) one can realize that the decay rate is enhanced when the system parameters do *not* fulfill the RET condition, i.e., in this case for $F_0 = 0.95$ and 1.5 . For the case of $F_0 = 1.25$ (RET) the tunneling rate is suppressed, and the symbols lie always below the reference line (dot-dot-dashed line). The enhancement is pronounced in the range of $\tau \approx 0.005 \dots 0.2 T_B$, corresponding to an energy scale equal or larger to than the band gap ΔE . On the other hand, for small values of the correlation time, the noise recovers

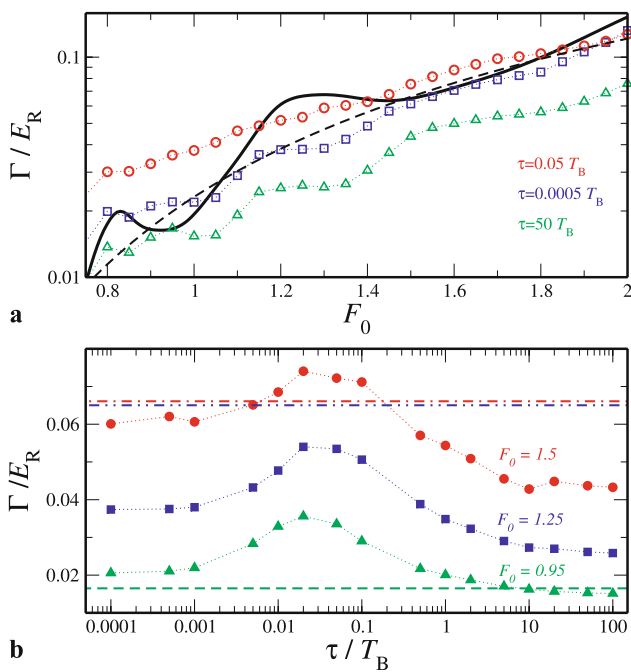


Fig. 5 The decay rate of the survival probability for $V_0 = 2.5 E_R$, and $D/\tau \approx 0.25$: **(a)** scan over F_0 for $\tau = 0.0005 T_B$ (open squares), $\tau = 0.05 T_B$ (open circles), $\tau = 50 T_B$ (open triangles), for the reference system (solid line), and the Landau-Zener exponential prediction for the reference system (dashed line); **(b)** scan over τ for $F_0 = 1.5$ (filled circles) and its reference system (dot-dot-dashed line), $F_0 = 1.25$ (filled squares) and its reference system (dot-dashed line), $F_0 = 0.95$ (filled triangles) and its reference system (dashed line)

the regime of white noise, where the effective potential describes the dynamics of the system very well, and for large values of τ , the system is in the regime of a slowly varying noise corresponding to energy scales that do not help to enhance the tunneling of atoms either.

3 Conclusion

It is possible to control the Landau-Zener (LZ) tunneling probability of the ultracold atoms from the ground band in tilted optical lattices. This control is possible by changing the system parameters such as the lattice depth and the Stark force, or by changing the initial condition which is given by the initial width of the momentum distribution of the BEC. All the mentioned parameters can be easily tuned experimentally. Furthermore, our calculations showed that atom-atom interactions affect the LZ tunneling probability and a repulsive interaction typically leads to an enhancement of the LZ tunneling of the ultracold atoms from the ground band. Most interestingly, our results demonstrate that it is also possible to control the tunneling by adding noise to the system. By changing the noise parameters, the tunneling probability can be enhanced or suppressed. The noise

can particularly enhance the tunneling probability when the system parameters are chosen far from the RET condition.

Acknowledgements We acknowledge funding by the Excellence Initiative by the German Research Foundation (DFG) through the Heidelberg Graduate School of Fundamental Physics (grant number GSC 129/1) and the Global Networks Mobility Measures. S.W. is grateful to the Heidelberg Academy of Sciences and Humanities for the Academy Award 2010 and to the Hengstberger Foundation for support by the Klaus-Georg and Sigrid Hengstberger Prize 2009. G.T. thanks the Landesgraduiertenförderung Baden-Württemberg for support.

References

1. L.D. Landau, Phys. Z. Sowjetunion **2**, 46 (1932)
2. C. Zener, Proc. R. Soc. A **137**, 696 (1932)
3. E.C.G. Stückelberg, Helv. Phys. Acta **5**, 369 (1932)
4. E. Majorana, Nuovo Cimento **9**, 43 (1932)
5. K. Leo, P.H. Bolivar, F. Brueggemann, R. Schwedler, K. Koehler, Solid State Commun. **84**, 943 (1992)
6. E. Peik, M. Ben Dahan, I. Bouchoule, Y. Castin, C. Salomon, Phys. Rev. A **55**, 2989 (1997)
7. M. Ben Dahan, E. Peik, J. Reichel, Y. Castin, C. Salomon, Phys. Rev. Lett. **76**, 4508 (1996)
8. S.R. Wilkinson, C.F. Bharucha, K.W. Madison, Q. Niu, M.G. Raizen, Phys. Rev. Lett. **76**, 4512 (1996)
9. S.R. Wilkinson, C.F. Bharucha, K.W. Madison, Q. Niu, M.G. Raizen, Nature (London) **387**, 575 (1997)
10. B.P. Anderson, M.A. Kasevich, Science **282**, 1686 (1998)
11. M. Glück, A.R. Kolovsky, H.J. Korsch, Phys. Rep. **366**, 103 (2002)
12. K. Leo, *High-Field Transport in Semiconductor Superlattices* (Springer, Berlin, 2003)
13. Q. Niu, M.G. Raizen, Phys. Rev. Lett. **80**, 3491 (1998)
14. O. Morsch, J.H. Müller, M. Cristiani, D. Ciampini, E. Arimondo, Phys. Rev. Lett. **87**, 140402 (2001)
15. G. Roati, E. de Mirandes, F. Ferlaino, H. Ott, G. Modugno, M. Inguscio, Phys. Rev. Lett. **92**, 230402 (2004)
16. O. Morsch, M. Oberthaler, Rev. Mod. Phys. **78**, 179 (2006)
17. I. Bloch, J. Dalibard, W. Zwerger, Rev. Mod. Phys. **80**, 885 (2008)
18. L. Santos, M.A. Baranov, J.I. Cirac, H.-U. Everts, H. Fehrmann, M. Lewenstein, Phys. Rev. Lett. **93**, 030601 (2004)
19. D. Clément, A.F. Varón, J.A. Retter, L. Sanchez-Palencia, A. Aspect, P. Bouyer, J. New, New J. Phys. **8**, 165 (2006)
20. L. Sanchez-Palencia, D. Clément, P. Lugan, P. Bouyer, A. Aspect, New J. Phys. **10**, 045019 (2008)
21. P. Lugan, D. Clément, P. Bouyer, A. Aspect, M. Lewenstein, L. Sanchez-Palencia, Phys. Rev. Lett. **98**, 170403 (2007)
22. T. Schulte, S. Drenkelforth, G. Kleine Büning, W. Ertmer, J. Arlt, M. Lewenstein, L. Santos, Phys. Rev. A **77**, 023610 (2008)
23. T. Salger, C. Geckeler, S. Kling, M. Weitz, Phys. Rev. Lett. **99**, 190405 (2007)
24. T. Salger, S. Kling, T. Hecking, C. Geckeler, L. Morales-Molina, M. Weitz, Science **326**, 1241 (2009)
25. M. Cristiani, O. Morsch, J.H. Müller, D. Ciampini, E. Arimondo, Phys. Rev. A **65**, 063612 (2002)
26. M. Jona-Lasinio, O. Morsch, M. Cristiani, N. Malossi, J.H. Müller, E. Courtade, M. Anderlini, E. Arimondo, Phys. Rev. Lett. **91**, 230406 (2003)
27. C. Sias, A. Zenesini, H. Lignier, S. Wimberger, D. Ciampini, O. Morsch, E. Arimondo, Phys. Rev. Lett. **98**, 120403 (2007)
28. A. Zenesini, C. Sias, H. Lignier, Y. Singh, D. Ciampini, O. Morsch, R. Mannella, E. Arimondo, A. Tomadin, S. Wimberger, New J. Phys. **10**, 053038 (2008)

29. A. Zenesini, H. Lignier, G. Tayebirad, J. Radogostowicz, D. Ciampini, R. Mannella, S. Wimberger, O. Morsch, E. Arimondo, *Phys. Rev. Lett.* **103**, 090403 (2009)
30. S. Wimberger, R. Mannella, O. Morsch, E. Arimondo, A.R. Kolovsky, A. Buchleitner, *Phys. Rev. A* **72**, 063610 (2005)
31. M. Holthaus, *J. Opt. B* **2**, 589 (2000)
32. G. Tayebirad, A. Zenesini, D. Ciampini, R. Mannella, O. Morsch, E. Arimondo, N. Lörch, S. Wimberger, *Phys. Rev. A* **82**, 013633 (2010)
33. G. Tayebirad, A. Zenesini, D. Ciampini, R. Mannella, O. Morsch, E. Arimondo, N. Lörch, S. Wimberger, *Phys. Rev. A* **82**, 069904 (2010)
34. P. Schlagheck, S. Wimberger, *App. Phys. B* **86**, 385 (2007)
35. M. Gustavsson, E. Haller, M.J. Mark, J.G. Danzl, G. Rojas-Kopeinig, H.-C. Nägerl, *Phys. Rev. Lett.* **100**, 080404 (2008)
36. A.R. Kolovsky, H.J. Korsch, E.-M. Graefe, *Phys. Rev. A* **80**, 023617 (2009)